Progress In Electromagnetics Research C, Vol. 43, 231–246, 2013

A TUNABLE HIGH IMPEDANCE SURFACE AND ITS APPLICATION TO DUAL-BAND MICROSTRIP ANTENNA

Ankush Gupta, Mahesh P. Abegaonkar*, Ananjan Basu, and Shiban K. Koul

Centre for Applied Research in Electronics, Indian Institute of Technology, Delhi, India

Abstract—This paper presents a simple method of tuning the AMC band of a high-impedance surface. The tunability is obtained with only two varactor diodes and a simple bias-network. The proposed structure, when used as a ground plane for a microstrip antenna, splits the resonance frequencies on the two sides of a reference antenna frequency. The resonance split is analyzed by employing cavity model and transmission line model of the patch antenna. Considerable tuning range is obtained in both the split bands. The simulated, measured and calculated results are found to be in good agreement.

1. INTRODUCTION

The trend in communication industry today is of reconfigurable and tunable systems. Systems can be reconfigured in terms of operating frequency, functionality, etc. Many of such systems require antennas that can work at more than one frequency. There have been numerous reports in the open-literature on reconfigurable antenna structures. Most of them employ PiN/Schottky diodes, FETs, RF MEMS switches, etc. Another approach for achieving tunability is by using tunable high-impedance surfaces (HIS)/Artificial Magnetic Conductor (AMC) [1]. Sievenpiper reported a leaky wave antenna using tunable HIS [2]. Other tunable antennas including tunable-HIS based are reported in [1, 3–18]. Most of these structures require a large number of active elements which translates into complexity of the biasing network and high cost for the tunable antenna. Recently,

Received 1 August 2013, Accepted 2 September 2013, Scheduled 9 September 2013

* Corresponding author: Mahesh P. Abegaonkar (mpjosh@care.iitd.ac.in).

attempts have been made to reduce the number of varactors in a tunable HIS. In [19], the authors report a technique to reduce the number of varactors required to synthesize a tunable HIS. In this technique, the HIS and the varactors are on two different substrates which may limit the practical usability of the tunable HIS. In this paper, we report a simple method to tune a finite HIS using varactor. The synthesized tunable HIS, when used as a ground plane for a microstrip antenna, results in resonance splitting. Each of these split bands can be tuned by varying voltage applied to the varactor.

2. DESIGN OF THE HIGH IMPEDANCE SURFACE

2.1. Initial Design

Various researchers have reported the use of EBG structure as Frequency Selective Surfaces (FSS). These structures have reflection characteristics such that they behave as artificial magnetic conductors over a band of frequencies, i.e., the incident wave and reflected wave are in phase with each other over the HIS band. In this work, a standard square patch was taken as the starting point for the ease of fabrication as well as analysis. The unit cell dimensions of the HIS structure were optimized for an arbitrarily chosen frequency 5 GHz, and a probe-fed reference patch antenna was designed for resonance within the HIS band. A substrate with a dielectric constant 2.2 and thickness 0.762 mm was used for both the patch antenna and the HIS layer. A 4×4 array of HIS surface was placed below the microstrip antenna thereby replacing the PEC ground by HIS/AMC ground. The microstrip antenna with HIS ground is shown in Fig. 1(a). The HIS band of the frequency selective surface was changed by incorporating

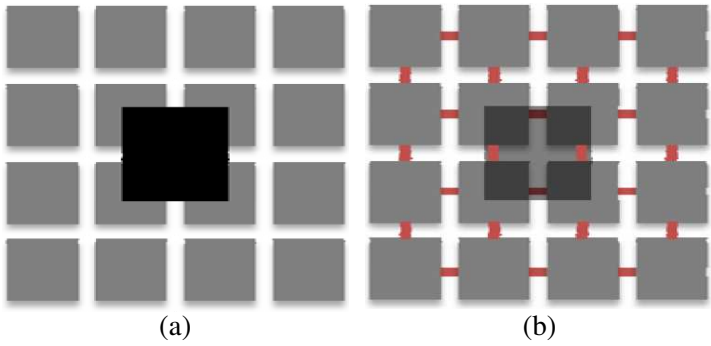

Figure 1. Patch antenna with AMC surface as ground. (a) Without shorting pins, (b) with shorting pins.

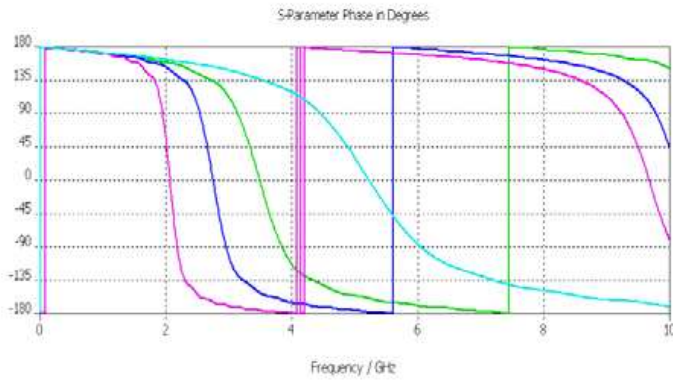

Figure 2. Reflection phase characteristics of AMC surface.

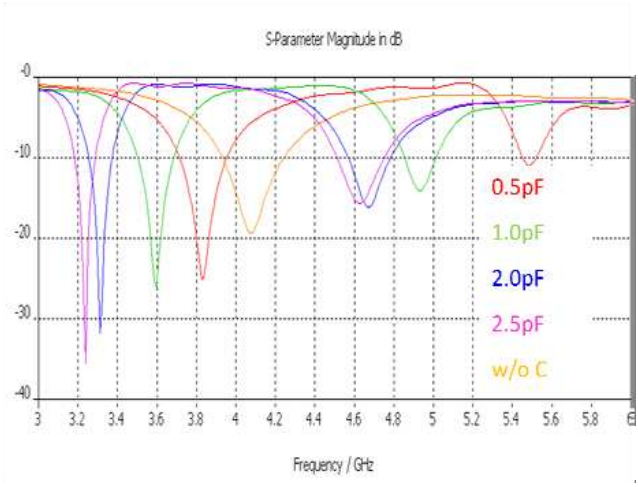

Figure 3. S_{11} for patch antenna using capacitors instead of shorting pins.

shorting pins (or capacitors) between the HIS patches (Fig. 1(b)).

To achieve tunability in the structure, the shorting pins were replaced with capacitors of different values, and it was observed that varying the capacitance form 0 pF to 2 pF varied the resonant frequency from 5 GHz to 2 GHz as shown in Fig. 2. The shift in the AMC point caused a similar shift in the resonant frequency of microstrip antenna. The simulated response of the antenna is shown in Fig. 3. It is also seen from Fig. 3 that the antenna is resonant at two frequencies: one below and one above the original frequency.

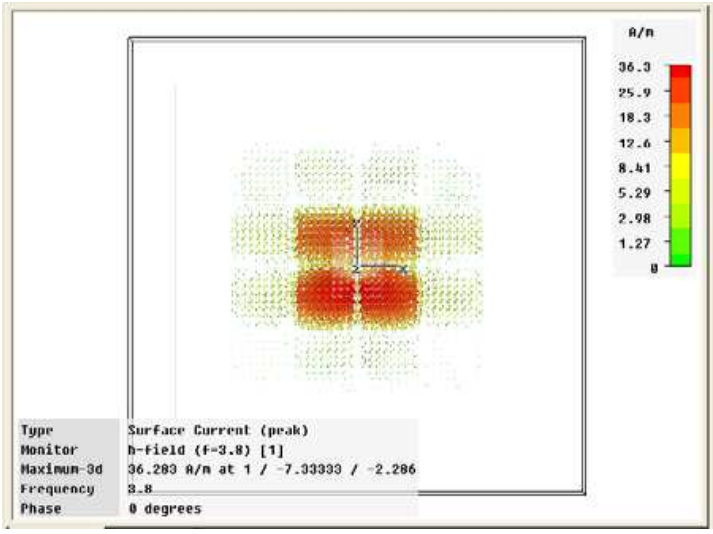

Figure 4. Current distribution on the AMC ground plane.

2.2. Simplified HIS Design

The probe fed microstrip antenna design consists of a ground plane, an air gap of 60 mils to accommodate the varactor diodes, a single layer of Rogers RO 4232 substrate and the patch on top. The length and width of the patch are 15 mm, and 21.5 mm respectively on 30 mils thick substrate over a 120 mm × 120 mm ($2\lambda \times 2\lambda$) ground plane. The reference antenna is designed to resonate at 5 GHz.

In order to make the final design physically implementable and at a very low cost, various simulations were carried out in CST Microwave studio to study the effect of variation in number of elements in the AMC layer on the resultant frequencies of the antenna system. The current patterns on the AMC ground plane were studied in order to analyze the cause of shifting of resonant frequency. Complete analysis has been discussed in subsequent sections. Fig. 4 shows the current distribution on the 4×4 array of patches on the AMC ground. Evidently, only the four central HIS patches have the maximum current density, hence it was hypothesized that eliminating the outer patches will not affect/degrade the performance of the antenna system. After further investigations, it was concluded that even a 2×2 array of patches as HIS layer would be able to provide the tunability, however, with slight reduction in the extent of tuning.

Although the response of the antenna system was satisfactory in

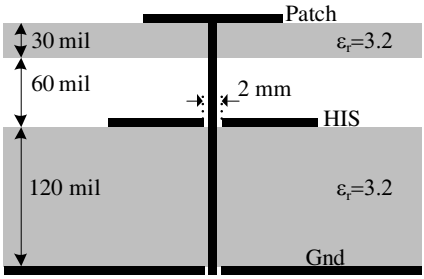

Figure 5. Cross section layout of antenna system.

the desired band of tuning, there were additional resonances observed in the return loss at certain higher frequency bands, and they were attributed to be originating from the patches in the AMC layer. In order to get these unwanted resonances out of the desired range, the thickness of the AMC was varied, and it was observed that with the increase in thickness the unwanted resonances shifted further out of the desired band. The proposed AMC layer consists of a 2×2 matrix of metallic square patches on a 120 mil thick Rogers RO 4232 layer as shown in Fig. 5. The HIS metal patches are with width 10 mm and periodicity 12 mm. Varactor diodes are mounted between the HIS patches in order to obtain the tuning in the patch antenna.

2.3. Design Using Varactor Diodes

Later, verifying the above results using fixed capacitor the incorporation of varactor diodes was attempted. The biasing lines were modeled in the AMC plane to cater for the DC biasing. Hyperabrupt tuning varactor diodes SMV-1232-079LF from Skyworks Inc. were used for the final design. The biasing circuit comprises two current limiting 10 kΩ resistors, and the final layout looks as that shown in Fig. 6. The effect of placement of biasing circuit was investigated by carrying out both near and far field measurements, and it was ascertained from experiments that the results do not deviate much after the incorporation of biasing circuit. The return loss S_{11} for the simulated and measured antenna with and without the biasing circuit is shown in Fig. 7.

Further experimentation on tunable antenna system revealed that only the capacitors across the radiating edges contribute to the shift in resonant frequency. This further simplified the circuit, and the AMC surface was slightly modified. The new AMC surface with biasing circuit is shown in Fig. 8.

The measured results of the antenna system with diodes mounted

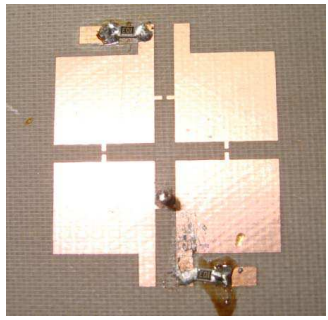

Figure 6. Fabricated AMC surface with biasing circuit.

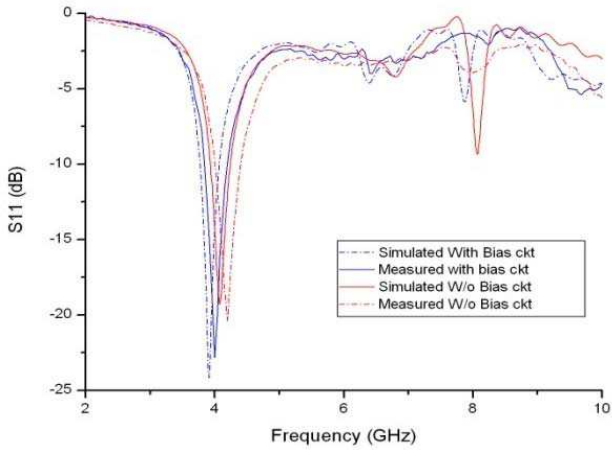

Figure 7. Return loss of antenna with AMC surface and biasing circuit.

on the AMC structure are shown in Fig. 9(a). There is a good agreement between the measured and simulated results as is evident from Fig. 9(b).

The radiation patterns at various frequencies were compared, and it was found that in the tuning range the patterns are considerably stable, and the 3 dB beam width remains constant. The E and H plane patterns at various frequencies are compared and shown in Figs. 10 and 11, respectively.

As seen from Fig. 9(b), there is a considerable difference between the measured and simulated return losses at the lower frequency when varactor capacitance is 4.15 pF. Moreover, the return loss at 2.9 GHz

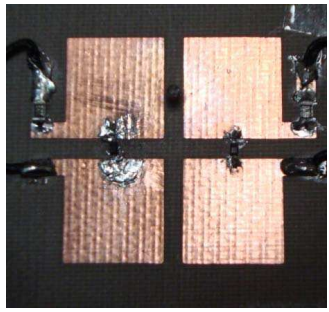

Figure 8. Fabricated modified AMC surface with biasing circuit.

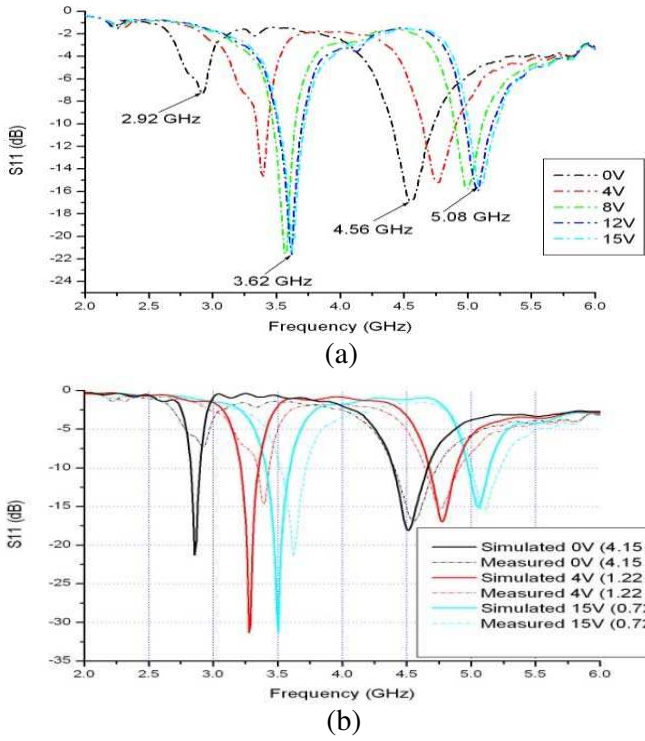

Figure 9. (a) Return loss of reconfigurable antenna with varactor diodes, (b) return loss of fabricated antenna vs. simulated results.

was found to be less than 10 dB, and the radiation pattern too was not in agreement with the simulated results. This difference was attributed to the fabrication errors and slight misplacement of the feed point. In

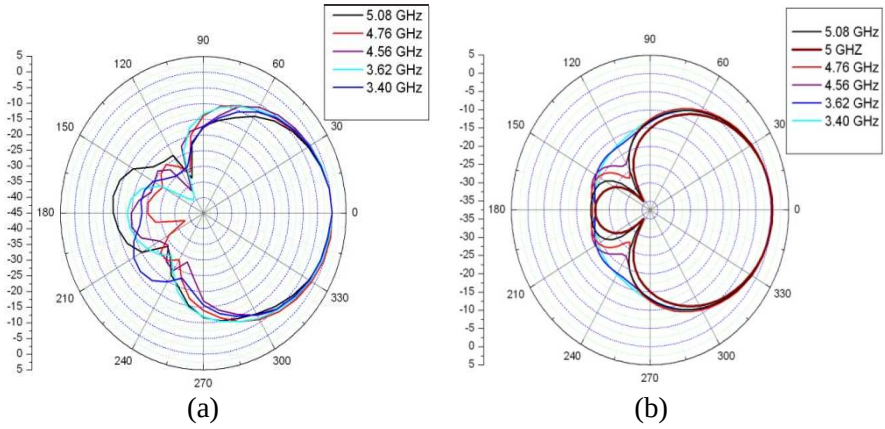

Figure 10. *H*-plane patterns of the antenna system. (a) Measured, (b) simulated.

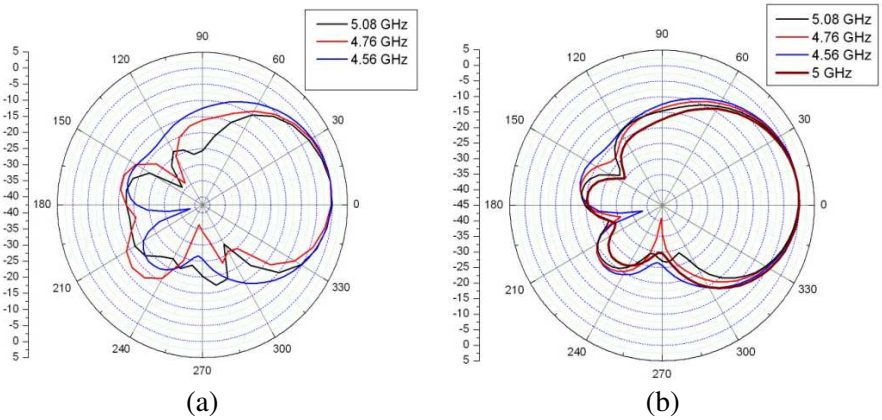

Figure 11. *E*-plane patterns of the antenna system. (a) Measured, (b) simulated.

order to keep the feed point at the same location and still change the feed point impedance, various antennas were fabricated with widths varying from 15 mm to 19 mm in steps of 2 mm. The antenna with 15 mm width was found to have return loss better than 10 dB. The return loss at various varactor biasing voltages is shown in Fig. 12. The radiation patterns at all the frequencies were measured again and found similar to that measured previously with exception at capacitance of 4.15 pF where measured results were found to match the simulated ones unlike in the previous case. The variation in the feed point impedance

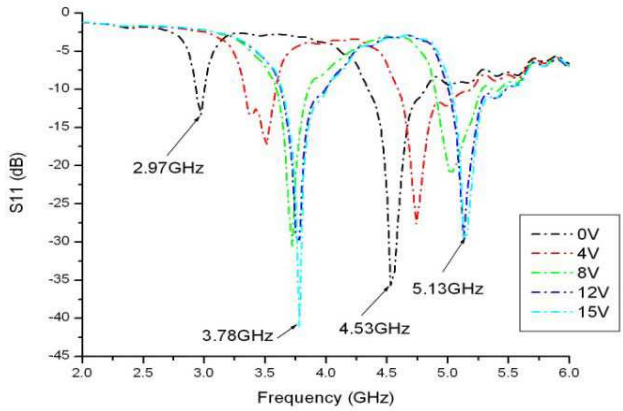

Figure 12. Return loss of reconfigurable antenna with varactor diodes.

resulted in the improvement of return loss beyond 10 dB. It however did not provide the reason for mismatch between the simulated and measured return losses at low frequency. The mismatch was finally traced to the resistance offered by the varactor diode. The resistance of the varactor varies with the applied voltage as well as the frequency of operation.

The varactor resistance too was then incorporated in the lumped component RLC model in CST microwave studio, and the results with additional resistance were compared with the measured results. The additional resistance of 1 Ohm was added to the simulation in order to cater for the resistance due to soldering and increase in resistance at high frequency. The measured response versus simulated one at 4.15 pF and 1.22 pF is shown in Fig. 13. As can be seen from the return loss plot, now there is a considerable agreement between the measured and simulated results.

3. ANALYSIS OF THE RESULTS

Analysis into the reasons for the suppression of original resonant frequency and origin of two new frequencies was carried out by monitoring the current and E field patterns of the patch at new resonant frequencies f_{lower} and f_{upper}. The current and E field patterns at patch antenna's original resonant frequency too were monitored. For analysis, the case of reference antenna with AMC surface without capacitor was used. In the present case, f_{lower} and f_{upper} are 4 GHz and 8 GHz, respectively. It was found that due to the presence of high

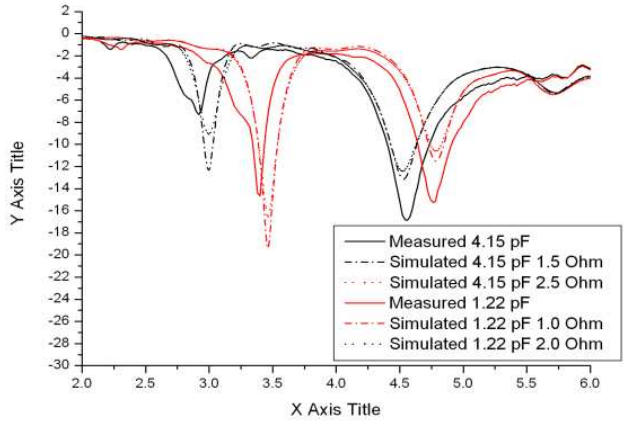

Figure 13. S_{11} of antenna system after incorporating series resistance of varactor.

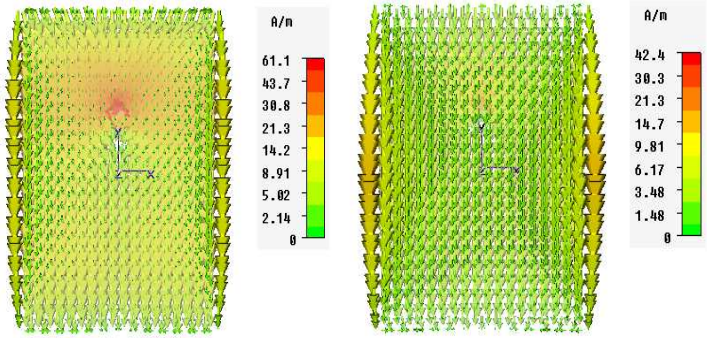

Figure 14. Current patterns on the patch. (a) 4 GHz, (b) 8 GHz.

impedance ground plane below the patch, the currents at 5 GHz were severely diminished leading to suppression of the resonant frequency of the patch antenna. The current pattern over the patch at two frequencies was found identical. Using the cavity model and the analogy of magnetic current over electric ground plane for a microstrip patch antenna, the E field patterns were analyzed. It was found that the E field patterns were almost identical for both the frequencies ruling out the possibility of generation of two different modes at the two frequencies. The current for the two frequencies is shown in Fig. 14. Both the patterns show a variation of only one half cycle at the two frequencies thereby indicating TM_{10} mode at f_{lower} as well as f_{upper}.

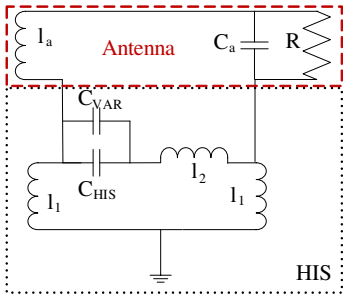

Figure 15. Equivalent circuit of patch antenna and high impedance surface.

In order to further analyze the reason for origin of two frequencies, the transmission line model and an equivalent RLC circuit for the antenna and the High impedance surface were used. The transmission line equivalent circuit of microstrip antenna is given in [20] and that of a high impedance surface given in [21, 22]. The same models have been used for analysis of the structure and stacked one on top of other as shown in Fig. 15. The high impedance surface loaded with varactor on top acts as variable high impedance surface which can be used to tune the patch antenna.

The imaginary component of the input admittance of the above equivalent circuit is given (1).

$$Y = \frac{\begin{array}{c} -j\left[\omega^4(2l_2c_al_1c_1 + 2l_ac_al_2c_1 + l_ac_al_1c_1)\right. \\ \left.-\omega^2(l_ac_a + 2l_2c_1 + 2l_2c_a + l_1c_1) + 1\right] \end{array}}{\begin{array}{c} \omega^5\left(l_al_1l_2c_1c_a + l_2^2l_1c_1c_a + l_2^2l_ac_1c_a\right) \\ +\omega^3\left(l_al_1c_1 + l_2l_1c_1 + l_2^2c_1 + 2l_al_2c_a + l_2^2c_1\right) + \omega(l_a + l_2) \end{array}} \tag{1}$$

Solve (1) for ω at resonance such that $Y = 0$ we get the expression for frequency of the antenna system at different capacitance values in the AMC surface as given in (2) and (3).

$$\omega = \sqrt{\frac{(l_ac_a + (2l_2 + l_1)c_1 + 2l_2c_a) \pm \sqrt{(l_ac_a + (2l_2 + l_1)c_1 + 2l_2c_a)^2 - 4(2l_2c_al_1c_1 + l_ac_a(2l_2 + l_1)c_1)}}{2(2l_2c_al_1c_1 + l_ac_a(2l_2 + l_1)c_1)}} \tag{2}$$

$$\omega = \sqrt{\frac{\left(\frac{1}{\omega_a^2} + \frac{1}{\omega_h^2} + 2l_2c_a\right) \pm \sqrt{\left(\frac{1}{\omega_a^2} + \frac{1}{\omega_h^2} + 2l_2c_a\right)^2 - 4\left(2l_2c_al_1c_1 + \frac{1}{\omega_a^2\omega_h^2}\right)}}{2\left(2l_2c_al_1c_1 + \frac{1}{\omega_a^2\omega_h^2}\right)}} \tag{3}$$

where,

ω = resonance frequency of antenna system.

ω_a = resonance frequency of reference antenna.

ω_h = center frequency of AMC surface.

l_a = inductance of patch antenna.

l_1 = inductance of AMC surface.

l_2 = inductance of dielectric substrate.

c_a = capacitance of patch antenna.

c_1 = capacitance of AMC surface.

Equation (3) proves the origin of two frequencies, viz. f_{lower} and f_{upper}, and suppression of original resonant frequency of the microstrip patch antenna. Circuit parameters for the reference antenna were extracted using standard equations available in the literature [20]. The Z parameters extracted from CST indicated the presence of significant probe inductance and capacitance. L_{probe} and C_{probe} were computed and found to be 1.9 nH and 2.798 pF, respectively.

The AMC structure simulated for reflection phase gives the response for an infinitely long high impedance surface. Hence the standard design equations cannot be used for computing the values of L and C of the AMC ground plane. Consequently, Equation (1) was used for computing L and C values of the finite HIS embedded between two dielectrics. The equivalent admittance was equated to zero to get the frequency at which the structure will start resonating

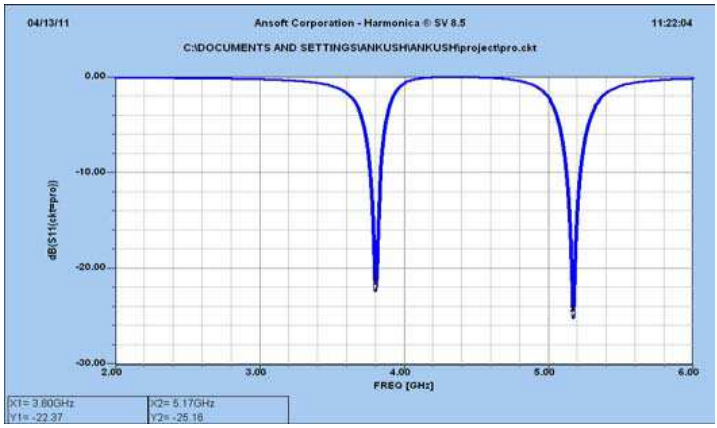

Figure 16. Simulated response in serenade.

Table 1. Comparison for calculated and measured results for various values of varactor capacitance. $L_S = 0.235\,\text{nH}$, $L_{\text{HIS}} = 0.068\,\text{nH}$, $C_{\text{HIS}} = 3.08\,\text{pF}$.

	Case I	**Case II**	**Case III**
C_{VAR} (pF)	0.72	1.22	4.15
f_{lower} predicted (GHz)	3.80	3.66	2.97
f_{lower} measured (GHz)	3.62	3.40	2.92
Offset (GHz)	+0.18	+0.26	0.05
f_{upper} predicted (GHz)	5.17	5.06	4.81
f_{upper} measured (GHz)	5.08	4.76	4.56
Offset (GHz)	+0.09	+0.30	+0.25

and was obtained in form of the following equation:

$$\omega^4(2l_2c_al_1c_1 + l_ac_a(2l_2 + l_1)c_1) \\ -\omega^2(l_ac_a + (2l_2 + l_1)c_1 + 2l_2c_a) + 1 = 0 \quad (4)$$

The above equation has three unknowns; l_1, C_1 ($C_{\text{HIS}} + C_{\text{var}}$), and l_2 thus one set of two frequencies generated by placement of varactor is not sufficient for solving the resulting simultaneous equation. Hence, two sets of frequencies obtained from extreme set of capacitances were used to obtain four equations from three unknowns. At $C_{\text{var}} = 4.15\,\text{pF}$, the measured frequencies were 2.92 GHz and 4.56 GHz, whereas at $C_{\text{var}} = 0.72\,\text{pF}$, the measured frequencies were 3.62 GHz and 5.08 GHz. Using the above set of equations, the lumped element values for the finite high impedance surface were obtained as $C_{\text{HIS}} = 3.0793\,\text{pF}$, $l_1 = 0.2351\,\text{nH}$, $l_2 = 0.0684\,\text{nH}$. The values were plugged into equivalent circuit made in serenade, and the resulting response was compared with the measured values. The return loss for varactor capacitance of 0.72 pF is shown in Fig. 16.

Similar graphs were obtained for other values of the varactor capacitance. A comparison of predicted and actual frequencies was carried out, and the results are as shown in Table 1.

4. CONCLUSION

A reconfigurable antenna system using finite artificial magnetic conductor which can be tuned in two different bands simultaneously has been proposed and verified experimentally in this paper. Varactor diodes have been successfully used and experimental results obtained have excellent match with the simulated results. The use of finite AMC ground plane has facilitated in a compact design and the use of only two varactor diodes thereby reducing the complexity of biasing circuit.

The lower band of tunability provides reduction in size of the patch enabling the patch to resonate even at lengths as low as 0.35λ. This provides an effective reduction of 40% in length of the microstrip antenna. The radiation patterns of the antenna have been measured and found to be considerably stable in entire tuning range. This has been attributed to the placement of the active components on the ground plane and not on the radiating element itself.

The antenna system has been analyzed using the cavity model, and the transmission line model and an equivalent circuit of the structure has been proposed. The lumped element equivalent values of the structure have been extracted and used for verification of the results obtained. The equations proposed in the paper satisfy the origin of two frequencies and tunability due to variation in the varactor capacitance.

ACKNOWLEDGMENT

The authors (MPA, AB and SKK) would like to thank Department of Science & Technology (DST), Govt. of India for the financial support.

REFERENCES

1. Bianconi, G., F. Costa, S. Genovesi, and A. Monorchio, "Optimal design of dipole antenna backed by finite high-impedance screen," *Progress In Electromagnetic Research C*, Vol. 18, 137–151, 2011.
2. Sievenpiper, D. F., "Forward and backward leaky wave radiation with large effective aperture from an electronically tunable surface," *IEEE Trans. on Antennas and Propag.*, Vol. 53, No. 1, 236–247, Jan. 2005.
3. Panayi, P., M. Al-Nuaimi, and I. Ivrissimtzis, "Tuning techniques for planar inverted-F antenna," *Electron. Lett.*, Vol. 37, No. 16, 1003–1004, 2001.
4. Kolsrud, A., M.-Y. Li, and K. Chang, "Dual-frequency electronically tunable CPW-fed CPS dipole antenna," *Electron. Lett.*, Vol. 34, No. 7, 609–611, 1998.
5. Behdad, N. and K. Sarabandi, "Dual-band reconfigurable antenna with a very wide tuning range," *IEEE Trans. on Antennas and Propag.*, Vol. 54, 409–416, Feb. 2006.
6. Kitatani, K. and S. Yamamoto, "Coaxial feed-type microstrip patch antenna with variable antenna height," *Electron. Commun. Jpn. (Part I: Communications)*, Vol. 87, No. 2, 10–16, 2004.
7. Aberle, J., S.-H. Oh, D. Auckland, and S. Rogers, "Reconfigurable antennas for wireless devices," *IEEE Antennas Propag. Mag.*, Vol. 45, No. 6, 148–154, 2003.

8. Karmakar, N., "Shorting strap tunable stacked patch PIFA," *IEEE Trans. on Antennas and Propag.*, Vol. 52, No. 11, 2877–2884, 2004.
9. Behdad, N. and K. Sarabandi, "A varactor-tuned dual-band slot antenna," *IEEE Trans. on Antennas and Propag.*, Vol. 54, No. 2, 401–408, 2006.
10. Anagnostou, D., G. Zheng, M. Chryssomallis, J. Lyke, G. Ponchak, J. Papapolymerou, and C. Christodoulou, "Design, fabrication, and measurements of an RF-MEMS-based self-similar reconfigurable antenna," *IEEE Trans. on Antennas and Propag.*, Vol. 54, 422–432, 2006.
11. Cetiner, B. A., H. Jafarkhani, J.-Y. Qian, H. J. Yoo, A. Grau, and F. de Flaviis, "Multifunctional reconfigurable MEMS integrated antennas for adaptive MIMO systems," *IEEE Commun. Mag.*, Vol. 42, No. 12, 62–70, 2004.
12. Al-Dahleh, R., C. Shafai, and L. Shafai, "Frequency-agile microstrip patch antenna using a reconfigurable MEMS ground plane," *Microw. Opt. Technol. Lett.*, Vol. 43, No. 1, 64–67, 2004.
13. Cetiner, B. A., J. Y. Qian, H. P. Chang, M. Bachman, G. P. Li, and F. de Flaviis, "Monolithic integration of RF MEMS switches with a diversity antenna on PCB substrate," *IEEE Trans. on Microw. Theory and Tech.*, Vol. 51, 332–335, Jan. 2003.
14. Jung, C. W., M. J. Lee, G. P. Li, and F. de Flaviis, "Reconfigurable scan-beam single-arm spiral antenna integrated with RF-MEMS switches," *IEEE Trans. on Antennas and Propag.*, Vol. 54, 455–463, Feb. 2006.
15. Liang, J. and H. Y. D. Yang, "Microstrip patch antennas on tunable electromagnetic band-gap substrates," *IEEE Trans. on Antennas and Propag.*, Vol. 57, No. 6, 1612–1617, Jun. 2009.
16. Costa, F., A. Monorchio, S. Talarico, and F. M. Valeri, "An active high impedance surface for low profile tunable and steerable antennas," *IEEE Antennas and Wireless Propag. Lett.*, Vol. 7, 676–680, 2008.
17. Sievenpiper, D. F., J. H. Schaffner, H. J. Song, R. Y. Loo, and G. Tangonan, "Two-dimensional beam steering using an electrically tunable impedance surface," *IEEE Trans. on Antennas and Propag.*, Vol. 51, No. 10, 2713–2722, Oct. 2003.
18. Mias, C. and J. H. Yap, "A varactor-tunable high impedance surface with a resistive-lumped-element biasing grid," *IEEE Trans. on Antennas and Propag.*, Vol. 55, No. 7, 1955–1962, Jul. 2007.

19. Costa, F., A. Monarchio, and G. P. Vastante, "Tunable high-impedance surface with a reduced number of varactors," *IEEE Antennas and Wireless Propag. Lett.*, Vol. 10, 11–13, 2011.
20. Garg, R., P. Bhartia, I. Bahl, and A. Ittipiboon, *Microstrip Antenna Design Handbook*, Artech House, Norwood, 2001.
21. Costa, F., A. Monorchio, and G. Manara, "An equivalent-circuit modeling of high impedance surfaces employing arbitrarily shaped FSS," *IEEE Antennas and Propagation Society International Symposium*, 852–855, Charleston, USA, 2009.
22. Costa, F., S. Genovesi, and A. Monorchio, "On the bandwidth of high-impedance frequency selective surfaces," *IEEE Antennas Wireless Propag. Lett.*, Vol. 8, 1341–1344, 2009.